

1 **Uncovering the hidden antibiotic potential of Cannabis**

2  
3

4 Maya A. Farha<sup>1,2, †</sup>, Omar M. El-Halfawy<sup>1,2,3, †</sup>; Robert T. Gale<sup>1,2</sup>; Craig R. MacNair<sup>1,2</sup>; Lindsey A.  
5 Carfrae<sup>1,2</sup>; Xiong Zhang<sup>1,2</sup>, Nicholas G. Jentsch<sup>1,2</sup>; Jakob Magolan<sup>1,2</sup>; Eric D. Brown<sup>1,2\*</sup>

6

7 <sup>1</sup> Department of Biochemistry and Biomedical Sciences, McMaster University, Hamilton, Ontario L8N  
8 3Z5, Canada

9 <sup>2</sup> Michael G. DeGroot Institute of Infectious Disease Research, McMaster University, Hamilton,  
10 Ontario, L8N 3Z5, Canada

11 <sup>3</sup> Microbiology and Immunology Department, Faculty of Pharmacy, Alexandria University,  
12 Alexandria, 21521, Egypt

13 \* To whom correspondence should be addressed (ebrown@mcmaster.ca)

14 † These authors contributed equally

15  
16

17

18

19

20

21

22

23

24

25 **Abstract**

26  
27  
28  
29  
30  
31  
32  
33  
34  
35  
36  
37  
38  
39  
40  
41  
42  
43  
44  
45  
46  
47  
48  
49  
50  
51  
52  
53  
54  
55  
56  
57  
58  
59  
60  
61

The spread of antimicrobial resistance continues to be a priority health concern worldwide, necessitating exploration of alternative therapies. *Cannabis sativa* has long been known to contain antibacterial cannabinoids, but their potential to address antibiotic resistance has only been superficially investigated. Here, we show that cannabinoids exhibit antibacterial activity against MRSA, inhibit its ability to form biofilms and eradicate stationary phase cells persistent to antibiotics. We show that the mechanism of action of cannabigerol is through targeting the cytoplasmic membrane of Gram-positive bacteria and demonstrate *in vivo* efficacy of cannabigerol in a murine systemic infection model caused by MRSA. We also show that cannabinoids are effective against Gram-negative organisms whose outer membrane is permeabilized, where cannabigerol acts on the inner membrane. Finally, we demonstrate that cannabinoids work in combination with polymyxin B against multi-drug resistant Gram-negative pathogens, revealing the broad-spectrum therapeutic potential for cannabinoids.

62 Public Health agencies around the globe have identified antimicrobial resistance as one of the  
63 most critical challenges of our time. The rapid and global spread of antimicrobial-resistant organisms in  
64 recent years has been unprecedented. So much so that the world health organization (WHO) published  
65 its first ever list of antibiotic-resistant "priority pathogens", made up of 12 families of bacteria that pose  
66 the greatest threat to human health<sup>1</sup>. Among them, *Staphylococcus aureus* is the leading cause of both  
67 healthcare and community-associated infections worldwide and a major cause for morbidity and  
68 mortality<sup>2</sup>, especially with the emergence and rapid spread of methicillin-resistant *S. aureus* (MRSA),  
69 which is resistant to all known  $\beta$ -lactam antibiotics<sup>3</sup>. Worse yet, resistance to vancomycin, linezolid  
70 and daptomycin has already been reported in MRSA clinical strains, compromising the therapeutic  
71 alternatives for life-threatening MRSA infections<sup>4</sup>. Further, antibiotic-resistant Gram-negative  
72 infections have increasingly become a pressing issue in the clinic. Indeed, of the bacteria highlighted  
73 by the WHO, 75% are Gram-negative organisms. Among the currently approved antibiotics, the latest  
74 discovery of a new drug class dates back to more than 30 years ago. The rapid loss of antibiotic  
75 effectiveness and diminishing pipeline beg for the exploration of alternative therapies.

76 *Cannabis* plants are important herbaceous species that have been used in folk medicine since  
77 the dawn of times. Increasing scientific evidence is accumulating for the efficacy of its metabolites in  
78 the treatment, for example, of epilepsy, Parkinson disease, analgesia, multiple sclerosis, Tourette's  
79 syndrome and other neurological diseases<sup>5</sup>. At a very nascent stage are investigations into the potential  
80 of cannabis metabolites as antibacterial therapies. To date, assessments of their antibacterial activity  
81 have been few and superficial. *In vitro* studies have shown cannabinoids inhibit the growth of Gram-  
82 positive bacteria, mostly *S. aureus*, with no detectable activity against Gram-negative organisms<sup>6-9</sup>,  
83 where the clinical need is highest. Further, the mechanism of action has remained elusive and there has  
84 been little validation of antibacterial activity *in vivo*.

85 Here, we show that cannabinoids exhibit antibacterial activity against MRSA, inhibit its ability  
86 to form biofilms and eradicate stationary phase cells persistent to antibiotics. We show that the  
87 mechanism of action of cannabigerol (CBG) is through targeting the cytoplasmic membrane of Gram-  
88 positive bacteria and demonstrate *in vivo* efficacy of CBG in a murine systemic infection model caused  
89 by MRSA. We also show that cannabinoids are effective against Gram-negative organisms whose outer  
90 membrane is permeabilized, where CBG acts on the inner membrane. Finally, we demonstrate that  
91 cannabinoids work in combination with polymyxin B against multi-drug resistant Gram-negative  
92 pathogens, revealing the broad-spectrum therapeutic potential for cannabinoids. In all, our findings

93 position cannabinoids as promising leads for antibacterial development that warrant further study and  
94 optimization.

95

## 96 **Results and Discussion**

97

98 We began our study investigating the antibacterial, anti-biofilm and anti-persister activity of a  
99 variety of commercially available cannabinoids, including the five major cannabinoids,  
100 cannabichromene (CBC), cannabidiol (CBD), cannabigerol (CBG), cannabinol (CBN), and  $\Delta^9$ -  
101 tetrahydrocannabinol (THC), as well as a selection of their carboxylic precursors (pre-cannabinoids)  
102 and other synthetic isomers (18 unique molecules total) against methicillin-resistant *S. aureus* (MRSA)  
103 (Supplementary Table 1). Susceptibility tests were conducted according to the Clinical and Laboratory  
104 Standards Institute (CLSI) protocol against MRSA USA300, a highly virulent and prevalent  
105 community-associated MRSA. Overall, antibacterial activities for the five major cannabinoids (and  
106 some of their synthetic derivatives) were in line with previously published work<sup>6-8</sup>. Seven molecules  
107 were potent antibiotics with minimum inhibitory concentration (MIC) values of 2  $\mu\text{g/mL}$ , including  
108 CBG, CBD, CBN, cannabichromenic acid (CBCA) and THC along with its  $\Delta^8$ - and exo-olefin  
109 regioisomers. We observed moderate loss of potency associated with the benzoic acid moiety (CBG,  
110 CBD, and THC were more potent than CBGA, CBDA, THCA) and when n-pentyl substituent was  
111 replaced with n-propyl (CBD and THC were superior to CBDV and THCV) (Supplementary Table 1).  
112 These two modifications appeared to have an additive detrimental effect on antibacterial activity  
113 (THCVA, CBDVA). Two other THC derivatives, ( $\pm$ ) 11-nor-9-carboxy- $\Delta^9$ -THC, and ( $\pm$ ) 11-hydroxy-  
114  $\Delta^9$ -THC, as well as cannabicylol were inactive at the highest concentrations screened (MIC > 32  
115  $\mu\text{g/mL}$ ) (Supplementary Table 1).

116 Biofilm formation by MRSA, typically on necrotic tissues and medical devices, is considered  
117 an important virulence factor influencing its persistence in both the environment and the host  
118 organism<sup>10</sup>. These highly structured surface-associated communities of MRSA are typically associated  
119 with increased resistance to antimicrobial compounds and are generally less susceptible to host immune  
120 factors. We assessed the ability of the various cannabinoids to inhibit the formation of biofilms by  
121 MRSA, using static abiotic solid-surface assays in which MRSA was treated with increasing  
122 concentrations of cannabinoids under conditions favouring biofilm formation (Supplementary Fig. 1).  
123 In all, the degree of inhibition of biofilm formation correlated with antibacterial activity; those  
124 cannabinoids with potent activity against MRSA strongly suppressed biofilm formation and vice versa  
125 (Supplementary Fig. 1, Supplementary Table 1). The five major cannabinoids clearly repressed MRSA  
126 biofilm formation, with CBG (Fig. 1a) exhibiting the most potent anti-biofilm activity. Indeed, as little

127 as 0.5 µg/mL (1/4 MIC) of CBG inhibited biofilm formation by ~50% (Fig. 1b). Thus, this experiment  
128 underlined the strong inhibitory effect of cannabinoids on biofilm formation; this sub-MIC level of  
129 CBG did not affect planktonic growth.

130 Another challenge in the treatment of MRSA infections is the formation of non-growing,  
131 dormant ‘persister’ subpopulations that exhibit high levels of tolerance to antibiotics<sup>11-13</sup>. Persister cells  
132 have a role in chronic and relapsing *S. aureus* infections<sup>14</sup> such as osteomyelitis<sup>15</sup>, and endocarditis<sup>16</sup>.  
133 Here, we evaluated the killing activity of a series of cannabinoids against persisters derived from  
134 stationary phase cells of MRSA USA300 (Supplementary Fig. 2). These have been previously shown to  
135 be tolerant to conventional antibiotics such as gentamicin, ciprofloxacin and vancomycin<sup>11, 17-18</sup>. In  
136 general, the anti-persister activity correlated with potency against actively dividing cells as determined  
137 by MIC assays (Supplementary Table 1). Again, CBG was the most potent cannabinoid against  
138 persisters, whereas oxacillin and vancomycin were ineffective at concentrations that otherwise kill  
139 actively dividing cells (Supplementary Fig. 2, Fig. 1c). More specifically, CBG killed persisters in a  
140 concentration-dependent manner starting at 5 µg/ml. Notably, CBG rapidly eradicated a population of  
141 ~10<sup>8</sup> CFU/ml MRSA persisters to below the detection threshold within 30 minutes of treatment (Fig.  
142 1c).

143 We selected CBG (Fig.1a) for further studies of mechanism and *in vivo* efficacy. Not only did  
144 CBG potently inhibit MRSA, repress biofilm formation (Fig. 1b) and effectively eradicate persister  
145 cells (Fig. 1c), but it is non-psychotropic, non-sedative and constitutes a component of *Cannabis* for  
146 which there is high therapeutic interest<sup>19</sup>. Further, we were also able to synthesize CBG efficiently  
147 from olivetol and geraniol, two inexpensive precursors, in one synthetic operation. We were cognisant  
148 that such facile synthetic access would enhance the potential for subsequent medicinal chemistry-based  
149 development efforts. We determined the MIC<sub>90</sub> of CBG against 96 clinical isolates of MRSA using the  
150 CLSI protocol. The corresponding frequency distribution of MICs is presented in Fig. 1d. Overall, the  
151 MICs ranged from 0.0625 – 8 µg/mL with a resulting MIC<sub>90</sub> of 4 µg/mL. This activity compares  
152 favourably with conventional antibiotics for these multi-drug resistant strains.

153 Given its growth inhibitory action on Gram-positive bacteria, we reasoned isolating resistant  
154 mutants to CBG would be a straightforward approach to gather insights into its bacterial target. Indeed,  
155 resistance mutations can often be mapped to a drug's molecular target<sup>20</sup>. To this end, MRSA was  
156 repeatedly challenged with various lethal concentrations of CBG, ranging from 2-16x MIC, to select  
157 for spontaneous resistance in MRSA (Fig. 2). No spontaneously resistant mutants were obtained,  
158 indicating a frequency of resistance less than 10<sup>-10</sup> for MRSA. We also attempted to allow MRSA  
159 bacteria to develop resistance to CBG by sequential subcultures via 15-day serial passage in liquid

160 culture containing sub-MIC concentrations of CBG and, again, no change in the MIC of CBG was  
161 detected (Fig. 2). While these experiments were unsuccessful probes of mechanism, they suggested  
162 very low rates of resistance for CBG, a highly desirable property for an antibiotic.

163 We turned to chemical genomic analysis to generate hypotheses for the target of CBG. Such  
164 studies can reveal patterns of sensitivity among genetic loci that are characteristic of the mechanism of  
165 action of an antibacterial compound<sup>21</sup>. We confirmed that the model Gram-positive bacterium *B.*  
166 *subtilis* was susceptible to CBG (MIC 2 µg/mL), and screened a CRISPR interference knockdown  
167 library, of all essential genes in *B. subtilis*<sup>22</sup> for further sensitization to CBG. In the absence of  
168 induction, relying on basal repression (which leads to a ~3-fold repression of the knockdown library<sup>22</sup>),  
169 we were unable to detect any knockdowns sensitized to sub-lethal concentrations of CBG (Fig. 2).  
170 Low-level induction identified some sensitive and some suppressing clones, however follow-on work  
171 with the individual knockdowns in liquid culture via full checkerboard analysis (combining xylose, the  
172 inducer, with CBG) failed to confirm sensitivity or suppression. In all, we were unable to identify *bona*  
173 *fide* chemical genetic interactions among essential genes of *B. subtilis* and CBG. We next aimed to  
174 query the non-essential gene subset, this time using the Nebraska Transposon Mutant Library, a  
175 sequence-defined transposon mutant library consisting of 1,920 strains, each containing a single  
176 mutation within a nonessential gene of CA-MRSA USA300<sup>23</sup>, again looking for genetic enhancers or  
177 suppressors to generate target hypotheses (Fig. 2, Supplementary Fig. 3a). While we were unable to  
178 uncover genetic suppressors at supra-lethal concentrations of CBG, we identified 41 transposons as  
179 sensitive across 3 different sub-lethal concentrations of CBG (Supplementary Table 2). Analysis of  
180 these transposons revealed a significant enrichment for genes encoding proteins that are localized at the  
181 cytoplasmic membrane (Supplementary Fig. 3b) and enrichment for genes encoding functions in  
182 processes that take place at the cytoplasmic membrane, such as cellular respiration and electron  
183 transport chain (Supplementary Fig. 3c). In all, chemical genomic profiling with CBG generally linked  
184 its activity to cytoplasmic membrane function.

185 The lack of clear targets among the essential gene products, the predominance of chemical  
186 genetic interactions linked to membrane function, and the difficulty generating resistant mutants,  
187 suggested that CBG might act on the cytoplasmic membrane of MRSA. Indeed, the propensity of  
188 membrane-active compounds to generate resistance is frequently low<sup>24</sup>. Further, the bacterial  
189 membrane is critical for cell function and survival, and is essential irrespective of the metabolic status  
190 of the cell, including non-growing and persisting cells<sup>24</sup>. The strong action of CBG on persister cells  
191 would be consistent with such a mode of action. Thus, we assessed the ability of CBG to disrupt  
192 membrane function using the membrane potential-sensitive probe, 3,3'-dipropylthiadicarbocyanine

193 iodide (DiSC<sub>3</sub>(5)). In DiSC<sub>3</sub>-loaded MRSA cells, CBG caused a dose-dependent increase in  
194 fluorescence that occurred at a concentration consistent with the MIC of CBG (Fig. 2). To probe the  
195 possibility that CBG selectively dissipated membrane potential ( $\Delta\psi$ ) component of proton motive  
196 force, we tested for synergy with sodium bicarbonate, a known perturbant of  $\Delta\text{pH}$ , that has been shown  
197 to synergize with molecules that reduce  $\Delta\psi$ <sup>25</sup>. A lack of synergy between these compounds suggested  
198 CBG disrupts the integrity of the cytoplasmic membrane (Supplementary Fig. 4).

199 Having established strong *in vitro* potency for CBG against MRSA, we next sought to evaluate  
200 the *in vivo* efficacy in a murine systemic infection model of MRSA. The effect of CBG on a systemic  
201 infection mediated by the CA-MRSA USA300 strain is shown in Fig. 3. Given that no signs of acute  
202 toxicity were reported in a pharmacokinetic study of 120-mg/kg doses of CBG<sup>26</sup>, we used a dose of 100  
203 mg/kg in this study. CBG displayed a significant reduction in bacterial burden in the spleen by a factor  
204 of 2.8- $\log_{10}$  in CFU compared to the bacterial titer seen with the vehicle ( $p < 0.001$ , Mann-Whitney *U*-  
205 test). Overall, CBG displayed promising levels of efficacy in the systemic infection model.

206 To date, antibacterial activity of cannabinoids against Gram-negative organisms has largely  
207 been ruled out, since reported MICs values fall in the 100-200  $\mu\text{g/mL}$  range<sup>7-8</sup>. We confirmed this,  
208 obtaining MICs  $>128 \mu\text{g/mL}$  for all of the tested cannabinoids against the model Gram-negative  
209 organism *Escherichia coli*. Given the observed action of CBG on the cytoplasmic membrane of MRSA,  
210 we reasoned that CBG (and other cannabinoids) might be equally effective on the Gram-negative  
211 counterpart, the inner membrane. Further, just as many antibacterial compounds fail to work against  
212 Gram-negative pathogens due to a permeability barrier<sup>27</sup>, we reasoned that low permeability across the  
213 outer membrane (OM) may be the reason for the poor efficacy of cannabinoids. Thus, we investigated  
214 the antibacterial profile of the five major cannabinoids against *E. coli*, where their permeation was  
215 facilitated through the OM by means of chemical perturbation. To this end, we set up checkerboard  
216 assays to assess the interaction of CBG (Fig. 4a) and the four other main cannabinoids (Supplementary  
217 Fig. 5) with the membrane perturbant, polymyxin B against *E. coli*. Remarkably, all five major  
218 cannabinoids gained potent activity in the presence of sub-lethal concentrations of polymyxin B.  
219 Indeed, all interactions were deemed synergistic (Fig. 4, Supplementary Fig. 5). For example, CBG,  
220 which was inactive against *E. coli* ( $>128 \mu\text{g/mL}$ ), was strongly potentiated when combined with a sub-  
221 lethal concentration of polymyxin B (1  $\mu\text{g/mL}$  in the presence of 0.062  $\mu\text{g/mL}$  polymyxin B). We  
222 further assessed whether OM perturbation by genetic means would lead to similar results by evaluating  
223 the activity of CBG against a number of strains where the OM was compromised (Fig. 4b). In an *E. coli*  
224  $\Delta\text{bamB}\Delta\text{tolC}$  deletion strain, which renders *E. coli* hyperpermeable to many small molecules, due to  
225 loss of BamB, a component of the  $\beta$ -barrel assembly machinery for OM proteins and TolC, the efflux

226 channel in the outer membrane, CBG had a MIC of 4  $\mu\text{g}/\text{mL}$ , on par with its Gram-positive activity.  
227 Similarly, in a hyperporinated,  $\Delta 9$  strain of *E. coli*, where a recombinant pore was introduced in the  
228 OM and all nine known TolC-dependent transporters deleted<sup>28</sup>, CBG activity became evident with a  
229 MIC of 8  $\mu\text{g}/\text{mL}$ . Finally, in an *Acinetobacter baumannii* deficient in lipooligosaccharide (LOS-),  
230 which effectively alters the permeability of the OM<sup>29</sup>, CBG activity was enhanced greater than 128-  
231 fold, resulting in a MIC value of 0.5  $\mu\text{g}/\text{mL}$ . Overall, these results suggest that cannabinoids face a  
232 permeability barrier in Gram-negative bacteria and further imply that cannabinoids inhibit a bacterial  
233 process present in Gram-negative pathogens, and likely common to that in Gram-positive pathogens.

234 To this end, we investigated whether CBG acted on the inner membrane (IM) of *E. coli* as well  
235 as the OM, presumably as a consequence of nonspecific membrane effects, as reported for many  
236 membrane-active agents. IM and OM permeability were determined, respectively, from ortho-  
237 Nitrophenyl- $\beta$ -galactoside (ONPG) and nitrocefin hydrolysis in an *E. coli* strain constitutively  
238 expressing a cytoplasmic  $\beta$ -galactosidase and a periplasmic  $\beta$ -lactamase while lacking the lactose  
239 permease, as described in the literature<sup>30</sup>. As shown in Fig. 4c, CBG specifically acted on the IM, and  
240 only in the presence of polymyxin B at a sub-lethal concentration that had minimal effects on the IM  
241 alone. We observed that CBG (+polymyxin B) induced major permeability changes in the inner  
242 membrane, indicated by a marked increase in optical density values due to ONPG hydrolysis as a result  
243 of unmasking the cytoplasmic  $\beta$ -galactosidase, which can only occur with destabilization of IM, was  
244 time dependent (Fig. 4c). CBG exhibited no action on the OM (Supplementary Fig. 6). Overall, the  
245 mechanism of bacterial killing by CBG in *E. coli* is likely loss of IM integrity and requires antecedent  
246 OM permeabilization.

247 Combination antibiotic therapy is becoming an increasingly attractive approach to combat  
248 resistance<sup>31</sup>. So too is the strategy of using an OM perturbing molecule to facilitate the permeation of  
249 compounds that are otherwise active only on Gram-positive bacteria<sup>32</sup>. We assessed the therapeutic  
250 potential of the adjuvant polymyxin B in combination with CBG to inhibit the growth of priority Gram-  
251 negative pathogens such as *A. baumannii*, *E. coli*, *Klebsiella pneumoniae*, and *Pseudomonas*  
252 *aeruginosa* (Fig. 4d). We employed conventional checkerboard assays to determine the interaction and  
253 potency of CBG and polymyxin B when used concurrently against various multi-drug resistant clinical  
254 isolates. In all cases, synergy was evident, suggesting the potential for combination therapy of the  
255 cannabinoids with polymyxin B against Gram-negative bacteria. Of note, the activity of CBG does not  
256 seem to be affected by antibiotic-resistance mechanisms that are limiting the use of other antibiotics  
257 and works effectively regardless of the susceptibility profile of the causative organism.



258 In summary, we have investigated the therapeutic potential of cannabinoids, and specifically  
259 CBG, through a comprehensive study of *in vitro* potency on biofilms and persisters, as well as  
260 mechanism of action studies and *in vivo* efficacy experiments. Most notably, we have uncovered the  
261 hidden broad-spectrum antibacterial activity of cannabinoids and demonstrated the potential of CBG  
262 against Gram-negative priority pathogens. Taken together, our findings lend credence to the idea that  
263 cannabinoids may be produced by *Cannabis sativa* as a natural defense against plant pathogens.  
264 Notwithstanding, cannabinoids are well-established as drug compounds that have favourable  
265 pharmacological properties in humans. The work presented here suggests that the cannabinoid  
266 chemotype represents an attractive lead for new antibiotic drugs.

267  
268 **Acknowledgements** This work was supported by a salary award to E.D.B from the Canada Research  
269 Chairs program and operating funds to E.D.B from a CIHR Foundation grant (FDN-143215); by  
270 a Michael G. DeGroot Centre for Medicinal Cannabis Research post-doctoral fellowship to O.M.E.  
271 Synthetic chemistry was supported by McMaster's Faculty of Health Sciences and the Michael G.  
272 DeGroot Institute for Infectious Disease Research.

273 **Author contributions** M.A.F., O.M.E., R.T.G., and E.D.B. conceived and designed the research.  
274 M.A.F. and O.M.E., performed all experiments and analyzed data with the exception of the mouse  
275 infection model and the synthesis of CBG. C.R.M. and L.A.C. performed the mouse infection model.  
276 X.Z. and N.G.J. optimized a scalable synthesis of CBG, supervised by J.M. M.A.F. and E.D.B. wrote  
277 the paper, with large input from O.M.E. All authors approved the final version.

278 **Competing interests** E.D.B., J.M., M.A.F., O.M.E., and R.T.G. are inventors on a patent application  
279 on the use of cannabinoids for prevention and/or treatment of infections.

## 280 METHODS

281 **Strains and reagents.** Supplemental Table 3 lists bacteria and plasmids used in this work. Bacteria  
282 were grown in cation-adjusted Mueller Hinton broth (CAMHB) at 37°C, unless otherwise stated.  
283 Cannabinoid standards and antibiotics were obtained from Sigma, Oakville, ON, Canada.

284 **Antimicrobial susceptibility testing.** Minimum inhibitory concentration (MIC) determination and  
285 checkerboard assays were conducted following the guidelines of CLSI for MIC testing by broth  
286 microdilution<sup>33</sup>. When accurate MIC values could not be determined, the highest concentration tested  
287 was considered to be half the MIC value. Fractional inhibitory concentration indices (FICI) were  
288 calculated as  $FICI = A/MIC_A + B/MIC_B$ , where A and B are the concentrations of two antibiotics  
289 required in combination to inhibit bacterial growth and  $MIC_A$  and  $MIC_B$  are the MIC values for drugs  
290 A and B alone<sup>34</sup>. FICI data were interpreted as 'synergy' ( $FICI \leq 0.5$ ), 'antagonism' ( $FICI > 4.0$ ), and  
291 'no interaction or indifference' ( $FICI 1-4.0$ ). Persister killing activity of cannabinoids was evaluated  
292 against stationary-phase cells of *S. aureus* as previously described<sup>35</sup>.

293 ***B. subtilis* CRISPRi essential gene knockdown strain collection screen.** Overnight cultures of the  
294 collection<sup>22</sup> (at a 96-well density,  $n = 289$ ) were performed using the Singer rotor HDA (Singer  
295 Instruments, United Kingdom) in CAMHB. Subsequently, CAMHB with or without CBG were  
296 inoculated using the singer rotor at 96-well density. These experiments were performed either in the  
297 presence of 0.05% xylose (allowing low level of *dcas9* expression) or with no xylose induction  
298 (basal *dcas9* expression). The plates were incubated at 37°C and OD<sub>600</sub> was read after 24 h.

299 ***S. aureus* Nebraska Transposon Mutant Library (NTML) screen.** Overnight cultures of the  
300 NTML<sup>23</sup> (at a 384-well density) were performed using the Singer rotor HDA (Singer Instruments,  
301 United Kingdom) in CAMHB containing erythromycin (5 µg/mL). Subsequently, CAMHB with or  
302 without CBG were inoculated using the singer rotor at 384-well density. The plates were incubated at  
303 37°C and OD<sub>600</sub> was read after 24 h. Cellular localization and functional (gene ontology, GO-term)  
304 enrichment analyses were performed using Pathway Tools software and MetaCyc database<sup>36</sup>.

305 **Selection of suppressor mutants of CBG activity in *S. aureus*.** Spontaneous suppressor mutants were  
306 selected for in liquid culture. Briefly, isolated colonies were resuspended in PBS and diluted to a final  
307 OD<sub>600</sub> of 0.05 into 200 µL of CAMHB containing CBG (at 4x and 8x MIC) set up in 96-well microtiter  
308 plates, 36 wells/concentration. Plates were incubated at 37°C for 4 days. Alternatively, bacteria were  
309 treated with a 2-fold series of CBG concentrations spanning the MIC. Bacteria growing at the  
310 maximum sub-MIC concentration were repeatedly passaged in a similar series of CBG concentrations  
311 by 1000-fold dilution every 24 hours. Five CBG dilution series were performed simultaneously and the  
312 cells were passaged for 15 days.

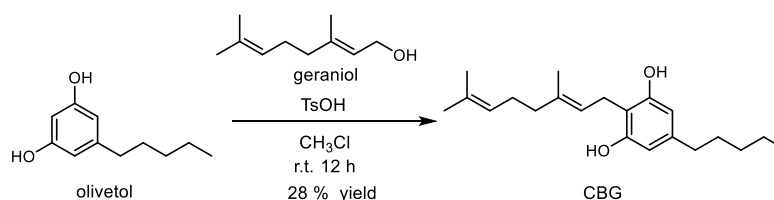
313 **General molecular techniques.** DNA manipulations were performed as previously described<sup>37</sup>. CaCl<sub>2</sub>  
314 chemically-competent ML35 cells were transformed with pBR322 encoding a periplasmic β-lactamase.

315 **Biofilm formation assays.** Biofilm formation was performed in polystyrene 96-well plates in Tryptic  
316 Soy Broth (TSB) with 1% glucose and detected by the crystal violet method as previously described<sup>38</sup>.

317 **Membrane integrity assays.** DiSC<sub>3(5)</sub> assay was performed in *S. aureus* as previously described<sup>39</sup>. To  
318 determine outer membrane and inner membrane activity of CBG against Gram-negative bacteria, we  
319 performed β-lactamase and β-galactosidase assays, respectively. Overnight cultures of ML35 pBR322  
320 in TSB with 50 µg/mL ampicillin were 100-fold diluted in fresh pre-warmed TSB and incubated at  
321 37°C at 220 rpm. Logarithmic phase cells were collected, washed twice in PBS and then resuspended in  
322 PBS at a final OD<sub>600</sub> of 0.01. Nitrocefin (30 µM) or ONPG (1.5 mM) - probes for β-lactamase and β-  
323 galactosidase, respectively (final concentration) - were added to the bacterial suspension and  
324 immediately aliquoted to dilution series of CBG and/or PMB at 100 µL final volume. Plates were  
325 incubated at 37°C and monitored kinetically for color change at 492 and 405 nm (for nitrocefin and  
326 ONPG hydrolysis, respectively). Adequate no drug, no probe and/or cell-free controls were included.

327 **Statistical analyses.** Statistical analyses were conducted with GraphPad Prism 5.0 and is indicated for  
328 each assay in the figure caption. All results are shown as mean ±SEM unless otherwise stated. In the  
329 case of MIC and checkerboard assays, the experiments were repeated at least three independent times  
330 and the experiment showing the most conservative effects (if applicable) was shown and the mean  
331 ±S.E.M. of the FICI was reported where applicable.

332 **Synthesis of Cannabigerol.** Chemical shifts in <sup>1</sup>H NMR and <sup>13</sup>C NMR spectra are reported in parts  
333 per million (ppm) relative to tetramethylsilane (TMS), with calibration of the residual chloroform peak  
334 at δ<sub>H</sub> 7.26, δ<sub>C</sub> 77.16. Peak multiplicities are reported using the following abbreviations: s, singlet; t,  
335 triplet; tq, triplet of quartets; m, multiplet. NMR spectra were recorded on a Bruker AVIII 700 NMR  
336 spectrometer. <sup>1</sup>H NMR spectra were acquired at 700 MHz with a default digital resolution (Bruker  
337 parameter: FIDRES) of 0.15 Hz/point, respectively. The <sup>13</sup>C NMR (DEPTq) spectrum provided shows  
338 CH and CH<sub>3</sub> carbon signals below the baseline and C and CH<sub>2</sub> carbons above the baseline. Olivetol  
339 was purchased from Oakwood Chemical. Geraniol was purchased from AK Scientific. All solvents  
340 and reagents were purchased from Fisher Scientific and used as received without further purification.  
341 Thin layer chromatography (TLC) was performed on Silicycle TLC plates (0.2 mm) pre-coated with  
342 silica gel F-254 and visualized by UV quenching and staining with *p*-anisaldehyde.  
343



344

345

346

347

348

349

350

351

352

353

354

355

356

357

358

359

360

361

362

363

364

365

366

367

368

369

370

371

CBG was synthesized using a reported procedure<sup>40</sup>. To a 25 mL round-bottomed flask containing a magnetic stir were added olivetol (108 mg, 0.6 mmol), chloroform (5 mL), geraniol (174  $\mu$ L, 1.0 mmol), *p*-toluene sulfonic acid monohydrate (19 mg, 0.1 mmol). The flask was covered with aluminum foil and the reaction was stirred at room temperature in the dark for 12 hours at which point TLC analysis indicated complete consumption of the olivetol substrate. To the reaction was added aqueous saturated NaHCO<sub>3</sub> (5 mL). The organic phase was removed and washed with water (5 mL). The aqueous layer was extracted with additional chloroform (5 mL) and the combined organic extracts were dried over MgSO<sub>4</sub> and concentrated *en vacuo*. The crude residue was purified via flash column chromatography on silica gel using gradient elution with hexanes and ethyl acetate. CBG was isolated as an off white powder in 28 % yield (54 mg, 0.17 mmol).

<sup>1</sup>H NMR (700 MHz, CDCl<sub>3</sub>)  $\delta$  6.25 (s, 2H), 5.28 (tq, J = 7.1, 1.3 Hz, 1H), 5.09 – 5.04 (m, 3H), 3.40 (d, J = 7.1 Hz, 2H), 2.49 – 2.43 (m, 2H), 2.14 – 2.04 (m, 4H), 1.82 (s, 3H), 1.68 (s, 3H), 1.60 (s, 3H), 1.58 – 1.54 (m, 2H), 1.36 – 1.28 (m, 4H), 0.89 (t, J = 7.0 Hz, 3H). <sup>13</sup>C NMR (176 MHz, CDCl<sub>3</sub>)  $\delta$  154.92, 142.89, 139.13, 132.19, 123.89, 121.84, 110.73, 108.52, 39.83, 35.65, 31.63, 30.93, 26.52, 25.81, 22.68, 22.40, 17.83, 16.32, 14.16.

**Mouse infection models.** Animal experiments were conducted according to guidelines set by the Canadian Council on Animal Care using protocols approved by the Animal Review Ethics Board at McMaster University under Animal Use Protocol #17-03-10. Before infection, mice were relocated at random from a housing cage to treatment or control cages. No animals were excluded from analyses, and blinding was considered unnecessary. Seven- to nine-week old female CD-1 mice (Envigo) were infected intraperitoneally with  $7.5 \times 10^7$  CFU of log-phase MRSA strain USA 300 JE2 with 5% porcine mucin. Treatment of 100 mg/kg CBG or a vehicle solution (60% PEG300 and 5% DMSO) were administered intraperitoneally immediately post-infection. Mice were euthanized 7 hours post-infection and tissues collected into phosphate buffered saline (PBS) at necropsy. Organs were homogenized using a high-throughput tissue homogenizer, serially diluted in PBS, and plated onto solid LB. Plates were incubated overnight at 37°C and colonies were quantified to determine organ load.

371

372

## References

373

374

375

376

377

378

379

380

381

382

383

384

385

386

387

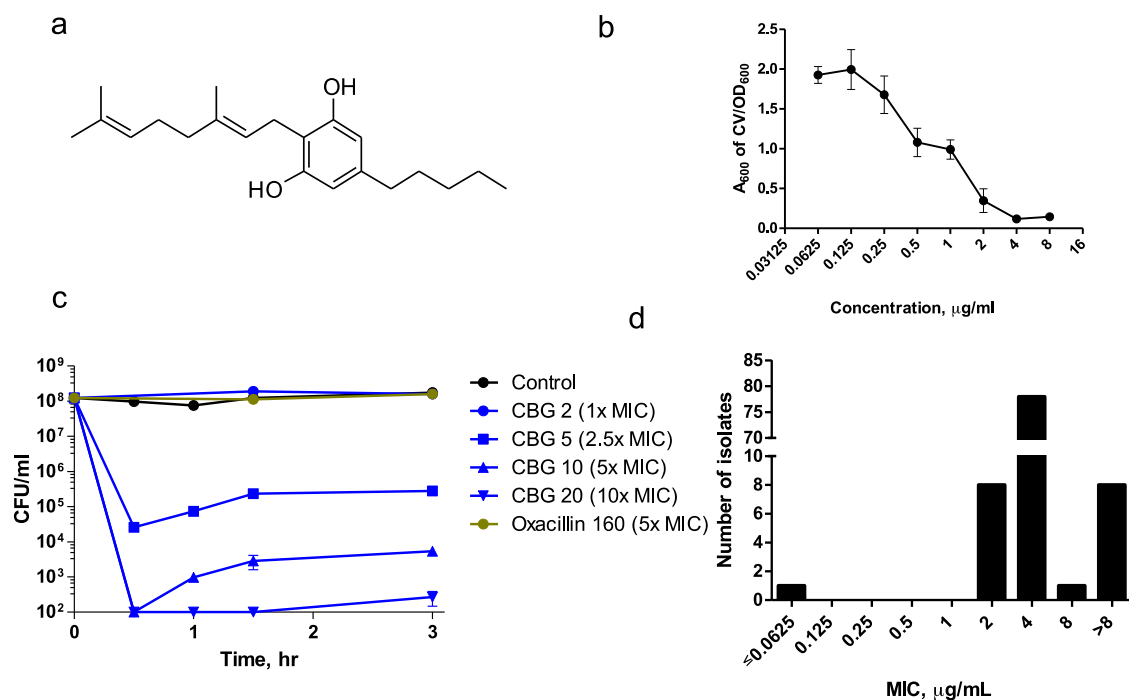
1. WHO *Global priority list of antibiotic-resistant bacteria to guide research, discovery, and development of new antibiotics*; World Health Organization: Geneva, 2017.
2. WHO *Prioritization of pathogens to guide discovery, research and development of new antibiotics for drug-resistant bacterial infections including tuberculosis*.; World Health Organization: Geneva, 2017.
3. Boucher, H. W.; Talbot, G. H.; Bradley, J. S.; Edwards, J. E.; Gilbert, D.; Rice, L. B.; Scheld, M.; Spellberg, B.; Bartlett, J., Bad bugs, no drugs: no ESKAPE! An update from the Infectious Diseases Society of America. *Clin Infect Dis* **2009**, *48* (1), 1-12. DOI: 10.1086/595011.
4. Nannini, E.; Murray, B. E.; Arias, C. A., Resistance or decreased susceptibility to glycopeptides, daptomycin, and linezolid in methicillin-resistant *Staphylococcus aureus*. *Current opinion in pharmacology* **2010**, *10* (5), 516-21. DOI: 10.1016/j.coph.2010.06.006.
5. Goncalves, J.; Rosado, T.; Soares, S.; Simao, A. Y.; Caramelo, D.; Luis, A.; Fernandez, N.; Barroso, M.; Gallardo, E.; Duarte, A. P., Cannabis and Its Secondary Metabolites: Their Use as Therapeutic Drugs, Toxicological Aspects, and Analytical Determination. *Medicines (Basel)* **2019**, *6* (1). DOI: 10.3390/medicines6010031.

- 388 6. Appendino, G.; Gibbons, S.; Giana, A.; Pagani, A.; Grassi, G.; Stavri, M.; Smith, E.; Rahman,  
389 M. M., Antibacterial cannabinoids from *Cannabis sativa*: a structure-activity study. *J Nat Prod* **2008**, *71*  
390 (8), 1427-30. DOI: 10.1021/np8002673.
- 391 7. Van Klingerden, B.; Ten Ham, M., Antibacterial activity of delta9-tetrahydrocannabinol and  
392 cannabidiol. *Antonie Van Leeuwenhoek* **1976**, *42* (1-2), 9-12.
- 393 8. Turner, C. E.; Elsohly, M. A., Biological activity of cannabichromene, its homologs and  
394 isomers. *J Clin Pharmacol* **1981**, *21* (S1), 283S-291S.
- 395 9. Blaskovich, M. A. T.; Kavanagh, A.; Ramu, S.; Levy, S.; Callahan, M.; Thurn, M., Cannabidiol  
396 is a Remarkably Active Gram-Positive Antibiotic. *ASM Microbe Conference*, San Francisco, California,  
397 2019.
- 398 10. Otto, M., Staphylococcal infections: mechanisms of biofilm maturation and detachment as  
399 critical determinants of pathogenicity. *Annu Rev Med* **2013**, *64*, 175-88. DOI: 10.1146/annurev-med-  
400 042711-140023.
- 401 11. Allison, K. R.; Brynildsen, M. P.; Collins, J. J., Metabolite-enabled eradication of bacterial  
402 persisters by aminoglycosides. *Nature* **2011**, *473* (7346), 216-20. DOI: 10.1038/nature10069.
- 403 12. Davies, J.; Davies, D., Origins and evolution of antibiotic resistance. *Microbiol Mol Biol Rev*  
404 **2010**, *74* (3), 417-33. DOI: 10.1128/MMBR.00016-10.
- 405 13. Lewis, K., Persister cells, dormancy and infectious disease. *Nat Rev Microbiol* **2007**, *5* (1), 48-  
406 56.
- 407 14. Conlon, B. P., *Staphylococcus aureus* chronic and relapsing infections: Evidence of a role for  
408 persister cells: An investigation of persister cells, their formation and their role in *S. aureus* disease.  
409 *Bioessays* **2014**, *36* (10), 991-6. DOI: 10.1002/bies.201400080.
- 410 15. Lew, D. P.; Waldvogel, F. A., Osteomyelitis. *Lancet* **2004**, *364* (9431), 369-79. DOI:  
411 10.1016/S0140-6736(04)16727-5.
- 412 16. Baddour, L. M.; Wilson, W. R.; Bayer, A. S.; Fowler, V. G., Jr.; Tleyjeh, I. M.; Rybak, M. J.;  
413 Barsic, B.; Lockhart, P. B.; Gewitz, M. H.; Levison, M. E.; Bolger, A. F.; Steckelberg, J. M.; Baltimore,  
414 R. S.; Fink, A. M.; O'Gara, P.; Taubert, K. A., Infective Endocarditis in Adults: Diagnosis, Antimicrobial  
415 Therapy, and Management of Complications: A Scientific Statement for Healthcare Professionals  
416 From the American Heart Association. *Circulation* **2015**, *132* (15), 1435-86. DOI:  
417 10.1161/CIR.0000000000000296.
- 418 17. Keren, I.; Kaldalu, N.; Spoering, A.; Wang, Y.; Lewis, K., Persister cells and tolerance to  
419 antimicrobials. *FEMS Microbiol Lett* **2004**, *230* (1), 13-8. DOI: S0378109703008565.
- 420 18. Conlon, B. P.; Rowe, S. E.; Gandt, A. B.; Nuxoll, A. S.; Donegan, N. P.; Zalis, E. A.; Clair, G.;  
421 Adkins, J. N.; Cheung, A. L.; Lewis, K., Persister formation in *Staphylococcus aureus* is associated  
422 with ATP depletion. *Nat Microbiol* **2016**, *1*, 16051. DOI: 10.1038/nmicrobiol.2016.51.
- 423 19. Andre, C. M.; Hausman, J. F.; Guerriero, G., *Cannabis sativa*: The Plant of the Thousand and  
424 One Molecules. *Front Plant Sci* **2016**, *7*, 19. DOI: 10.3389/fpls.2016.00019.
- 425 20. Zheng, X. S.; Chan, T. F.; Zhou, H. H., Genetic and genomic approaches to identify and study  
426 the targets of bioactive small molecules. *Chem Biol* **2004**, *11* (5), 609-18. DOI:  
427 10.1016/j.chembiol.2003.08.011.
- 428 21. Barker, C. A.; Farha, M. A.; Brown, E. D., Chemical genomic approaches to study model  
429 microbes. *Chem Biol* **2010**, *17* (6), 624-32. DOI: 10.1016/j.chembiol.2010.05.010.
- 430 22. Peters, J. M.; Colavin, A.; Shi, H.; Czarny, T. L.; Larson, M. H.; Wong, S.; Hawkins, J. S.; Lu,  
431 C. H. S.; Koo, B. M.; Marta, E.; Shiver, A. L.; Whitehead, E. H.; Weissman, J. S.; Brown, E. D.; Qi, L.  
432 S.; Huang, K. C.; Gross, C. A., A Comprehensive, CRISPR-based Functional Analysis of Essential  
433 Genes in Bacteria. *Cell* **2016**, *165* (6), 1493-1506. DOI: 10.1016/j.cell.2016.05.003.
- 434 23. Fey, P. D.; Endres, J. L.; Yajjala, V. K.; Widhelm, T. J.; Boissy, R. J.; Bose, J. L.; Bayles, K.  
435 W., A genetic resource for rapid and comprehensive phenotype screening of nonessential  
436 *Staphylococcus aureus* genes. *MBio* **2013**, *4* (1), e00537-12. DOI: 10.1128/mBio.00537-12.
- 437 24. Hurdle, J. G.; O'Neill, A. J.; Chopra, I.; Lee, R. E., Targeting bacterial membrane function: an  
438 underexploited mechanism for treating persistent infections. *Nat Rev Microbiol* **2011**, *9* (1), 62-75.  
439 DOI: 10.1038/nrmicro2474.

- 440 25. Farha, M. A.; French, S.; Stokes, J. M.; Brown, E. D., Bicarbonate Alters Bacterial  
441 Susceptibility to Antibiotics by Targeting the Proton Motive Force. *ACS Infect Dis* **2018**, *4* (3), 382-390.  
442 DOI: 10.1021/acsinfectdis.7b00194.
- 443 26. Deiana, S.; Watanabe, A.; Yamasaki, Y.; Amada, N.; Arthur, M.; Fleming, S.; Woodcock, H.;  
444 Dorward, P.; Pigliacampo, B.; Close, S.; Platt, B.; Riedel, G., Plasma and brain pharmacokinetic  
445 profile of cannabidiol (CBD), cannabidivarin (CBDV), Delta(9)-tetrahydrocannabivarin (THCV) and  
446 cannabigerol (CBG) in rats and mice following oral and intraperitoneal administration and CBD action  
447 on obsessive-compulsive behaviour. *Psychopharmacology (Berl)* **2012**, *219* (3), 859-73. DOI:  
448 10.1007/s00213-011-2415-0.
- 449 27. Delcour, A. H., Outer membrane permeability and antibiotic resistance. *Biochim Biophys Acta*  
450 **2009**, *1794* (5), 808-16. DOI: 10.1016/j.bbapap.2008.11.005.
- 451 28. Krishnamoorthy, G.; Wolloscheck, D.; Weeks, J. W.; Croft, C.; Rybenkov, V. V.; Zgurskaya, H.  
452 I., Breaking the Permeability Barrier of Escherichia coli by Controlled Hyperporination of the Outer  
453 Membrane. *Antimicrob Agents Chemother* **2016**, *60* (12), 7372-7381. DOI: 10.1128/AAC.01882-16.
- 454 29. Powers, M. J.; Trent, M. S., Expanding the paradigm for the outer membrane: Acinetobacter  
455 baumannii in the absence of endotoxin. *Mol Microbiol* **2018**, *107* (1), 47-56. DOI: 10.1111/mmi.13872.
- 456 30. Lehrer, R. I.; Barton, A.; Ganz, T., Concurrent assessment of inner and outer membrane  
457 permeabilization and bacteriolysis in E. coli by multiple-wavelength spectrophotometry. *J Immunol*  
458 *Methods* **1988**, *108* (1-2), 153-8.
- 459 31. Worthington, R. J.; Melander, C., Combination approaches to combat multidrug-resistant  
460 bacteria. *Trends Biotechnol* **2013**, *31* (3), 177-84. DOI: 10.1016/j.tibtech.2012.12.006.
- 461 32. Stokes, J. M.; MacNair, C. R.; Ilyas, B.; French, S.; Cote, J. P.; Bouwman, C.; Farha, M. A.;  
462 Sieron, A. O.; Whitfield, C.; Coombes, B. K.; Brown, E. D., Pentamidine sensitizes Gram-negative  
463 pathogens to antibiotics and overcomes acquired colistin resistance. *Nat Microbiol* **2017**, *2*, 17028.  
464 DOI: 10.1038/nmicrobiol.2017.28.
- 465 33. CLSI, *Methods for Dilution Antimicrobial Susceptibility Tests for Bacteria That Grow*  
466 *Aerobically; Approved Standard—Ninth Edition. CLSI document M07-A9.* Clinical and Laboratory  
467 Standards Institute: Wayne, PA, 2012.
- 468 34. Vaara, M.; Porro, M., Group of peptides that act synergistically with hydrophobic antibiotics  
469 against gram-negative enteric bacteria. *Antimicrob. Agents Chemother.* **1996**, *40* (8), 1801-1805.
- 470 35. Kim, W.; Zhu, W.; Hendricks, G. L.; Van Tyne, D.; Steele, A. D.; Keohane, C. E.; Fricke, N.;  
471 Conery, A. L.; Shen, S.; Pan, W.; Lee, K.; Rajamuthiah, R.; Fuchs, B. B.; Vlahovska, P. M.; Wuest, W.  
472 M.; Gilmore, M. S.; Gao, H.; Ausubel, F. M.; Mylonakis, E., A new class of synthetic retinoid antibiotics  
473 effective against bacterial persisters. *Nature* **2018**, *556* (7699), 103-107. DOI: 10.1038/nature26157.
- 474 36. Caspi, R.; Billington, R.; Fulcher, C. A.; Keseler, I. M.; Kothari, A.; Krummenacker, M.;  
475 Latendresse, M.; Midford, P. E.; Ong, Q.; Ong, W. K.; Paley, S.; Subhraveti, P.; Karp, P. D., The  
476 MetaCyc database of metabolic pathways and enzymes. *Nucleic Acids Res* **2018**, *46* (D1), D633-  
477 D639. DOI: 10.1093/nar/gkx935.
- 478 37. Sambrook, J.; Fritsch, E. F.; Maniatis, T., *Molecular cloning: a laboratory manual.* 2nd ed.;  
479 Cold Spring Harbor Laboratory: Cold Spring Harbor, New York, 1990.
- 480 38. Merritt, J. H.; Kadouri, D. E.; O'Toole, G. A., Growing and analyzing static biofilms. *Curr Protoc*  
481 *Microbiol* **2005**, *Chapter 1*, Unit 1B 1. DOI: 10.1002/9780471729259.mc01b01s00.
- 482 39. Farha, M. A.; Verschoor, C. P.; Bowdish, D.; Brown, E. D., Collapsing the proton motive force  
483 to identify synergistic combinations against *Staphylococcus aureus*. *Chem Biol* **2013**, *20* (9), 1168-78.  
484 DOI: 10.1016/j.chembiol.2013.07.006.
- 485 40. Taura, F.; Morimoto, S.; Shoyama, Y., Purification and characterization of cannabidiolic-acid  
486 synthase from Cannabis sativa L.. Biochemical analysis of a novel enzyme that catalyzes the  
487 oxidocyclization of cannabigerolic acid to cannabidiolic acid. *J Biol Chem* **1996**, *271* (29), 17411-6.  
488 DOI: 10.1074/jbc.271.29.17411.

489

490



491

492

493 **Fig. 1.** Cannabigerol (CBG) is a potent antibacterial, anti-biofilm and anti-persister cannabinoid. **a**, Chemical  
 494 structure of CBG **b**, Concentration dependence for inhibition of MRSA biofilm formation by CBG. Shown is the  
 495 average  $A_{600nm}$  measurements of crystal violet stained biofilms and normalized by the  $OD_{600}$  of planktonic cells  
 496 with error bars representing one standard error of the mean, S.E.M. ( $n=4$ ). **c**, Time-kill curve of *S. aureus*  
 497 USA300 persisters by CBG compared to oxacillin shown as mean  $\pm$ S.E.M ( $n=4$ ). CBG rapidly eradicated a  
 498 population of  $\sim 10^8$  CFU/ml MRSA persisters to below the detection threshold within 30 minutes of treatment .  
 499 On the other hand, the  $\beta$ -lactam oxacillin at 160  $\mu$ g/mL (5x MIC) did not show any activity against the same  
 500 population of persisters. **d**,  $MIC_{90}$  distribution of CBG against clinical isolates of MRSA ( $n=96$ ). The  $MIC_{90}$  is 4  
 501  $\mu$ g/mL.

502

503

504

505

506

507

508

509

510

511  
512  
513  
514  
515  
516  
517  
518  
519  
520  
521  
522  
523  
524  
525  
526  
527  
528  
529  
530  
531  
532  
533  
534  
535  
536  
537  
538  
539

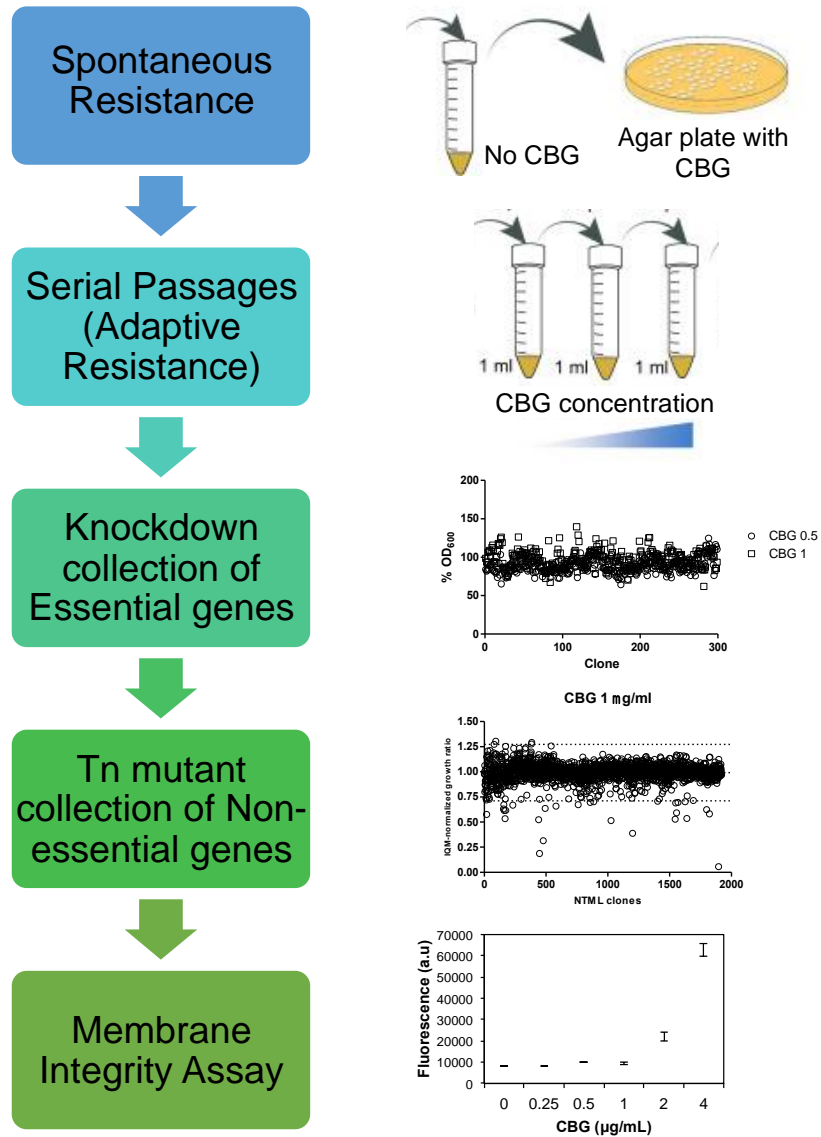


**Fig. 2.** CBG is active on the cytoplasmic membrane of MRSA. Overview of strategies for mechanism of action determination, culminating in the finding that CBG is active on the cytoplasmic membrane, as determined by dose-dependent increases in DiSC<sub>3</sub>(5) fluorescence.

540  
541  
542  
543  
544  
545  
546  
547  
548  
549  
550  
551  
552  
553  
554  
555  
556  
557  
558  
559  
560  
561  
562  
563  
564  
565  
566  
567  
568

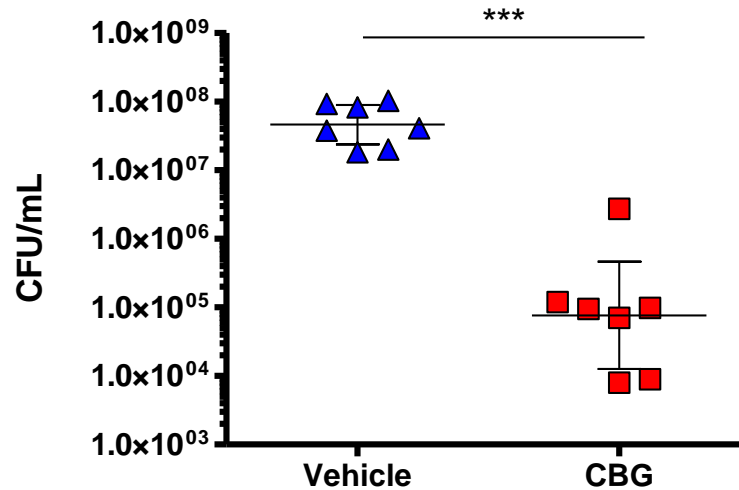
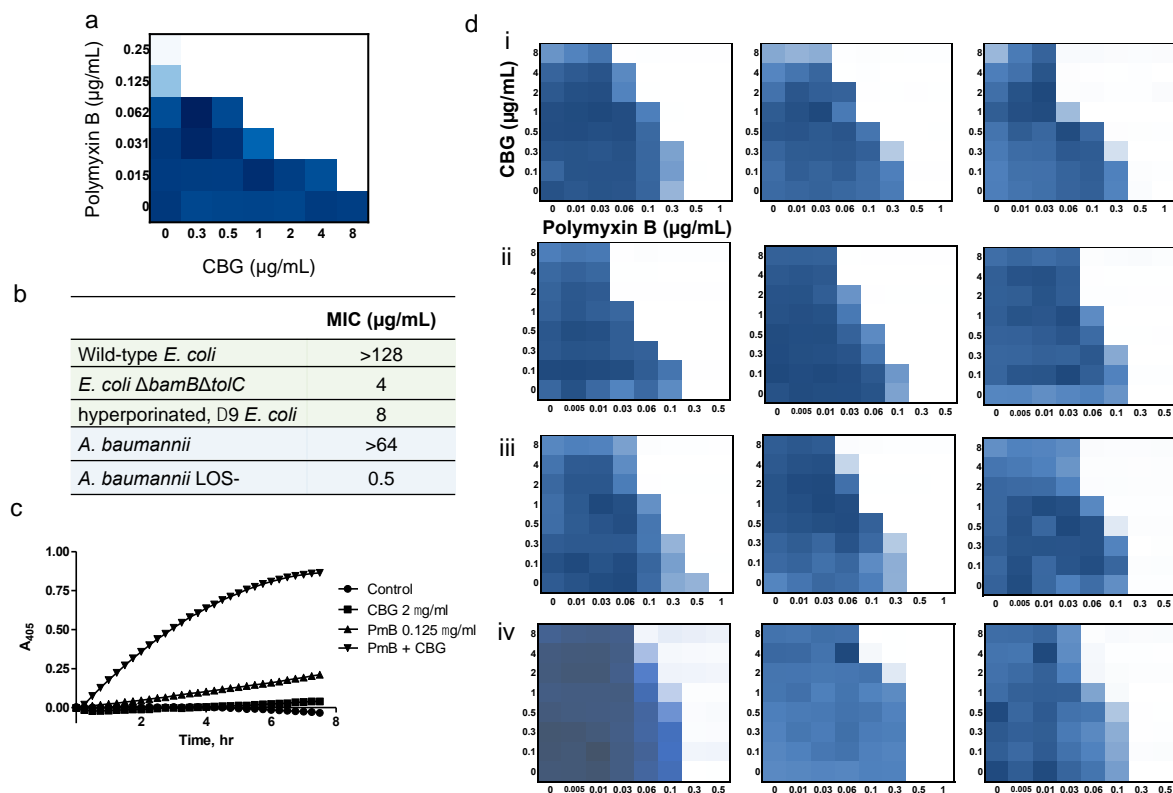


**Fig. 3.** CBG is efficacious in a systemic mouse model of *S. aureus* infection when administered single-dose treatment immediately post infection of CBG (n=7, red, 100 mg kg<sup>-1</sup>, i.p.) or vehicle control (n=7, blue, i.p.). Colony-forming units (CFU) within spleen tissue were enumerated at 7 h post infection. Horizontal lines represent the geometric mean of the bacterial load for each treatment group. Administration of CBG resulted in a 2.8-log<sub>10</sub> reduction ( $p < 0.001$ , Mann–Whitney *U*-test) in CFU when compared to the vehicle control.





569

570

571 **Fig. 4.** CBG is active against Gram-negative bacteria whose outer membrane is permeabilized, where it acts on  
 572 the inner membrane. **a**, Checkerboard analysis of CBG in combination with polymyxin B against *E. coli*. The  
 573 extent of inhibition is shown as a heat plot, such that the darkest blue color represents full bacterial growth. **b**,  
 574 CBG becomes active against Gram-negative bacteria in various genetic backgrounds where the outer membrane  
 575 is compromised. **c**, CBG acts on the IM of *E. coli* but only in the presence of sub-lethal concentration of  
 576 polymyxin B (PmB), unmasking cytoplasmic  $\beta$ -galactosidase leading to hydrolysis of ONPG as detected via  
 577 absorbance reads at 405 nm over time. **d**, CBG in combination with polymyxin B against multi-drug resistant  
 578 clinical isolates of i, *A. baumannii*, ii, *E. coli*, iii, *K. pneumoniae*, iv, *P. aeruginosa*. The extent of inhibition is  
 579 shown as a heat plot, such that the darkest blue color represents full bacterial growth.

580

581

582

583

584

585

586